Clinical and Experimental Immunology ORIGINAL ARTICLE doi: 10.1111/cei.13309

Disrupted regulation of serpinB9 in circulating T cells is associated with an increased risk for post-transplant skin cancer

F. S. Peters ,* A. M. A. Peeters,* T. P. P. van den Bosch,† A. L. Mooyaart,† J. van de Wetering,* M. G. H. Betjes,* C. C. Baan* and K. Boer*

*Rotterdam Transplant Group, Department of Internal Medicine, Erasmus MC, Erasmus University Medical Center, and †Department of Pathology, Erasmus MC, Erasmus University Medical Center, Rotterdam, the Netherlands

Accepted for publication 22 April 2019
Correspondence: F. S. Peters MSc, Rotterdam Transplant Group, Department of Internal Medicine, Erasmus MC, Erasmus University Medical Center, Postbus 2040, 3000 CA Rotterdam, the Netherlands.
E-mail: f.s.peters@erasmusmc.nl

Summary

Cutaneous squamous cell carcinoma (cSCC) is a serious complication after organ transplantation and patients benefit from an early risk assessment. We hypothesized that functional differences in circulating T cells may represent risk factors for post-transplant cSCC development. Here, we analysed genome-wide DNA methylation of circulating T cells of kidney transplant recipients before the clinical onset of cSCC, to identify differences associated with post-transplant cSCC development. This analysis identified higher DNA methylation of *SERPINB9*, which is an intracellular inhibitor of granzyme B, a protein that induces apoptosis in target cells. High DNA methylation of *SERPINB9* in circulating T cells was confirmed in a second patient cohort during recurrent cSCC, indicating that high *SERPINB9* methylation represents a persistent risk factor for cSCC development. At the functional level, the inverse correlation between DNA methylation and messenger RNA expression present in non-cSCC patients was absent in the cSCC patients. Also, a significant difference in serpinB9 protein expression between cSCC patients and non-cSCC patients was observed. It was concluded that disturbed regulation of serpinB9 in circulating T cells represents a novel risk factor for post-transplant cSCC in kidney transplant recipients.

Keywords: cutaneous squamous cell carcinoma, DNA methylation, epigenetics, kidney transplantation, PI-9

Introduction

Immunosuppression after organ transplantation is associated with a higher prevalence of cancer [1,2]. Non-melanoma skin cancer, in particular, such as cutaneous squamous cell carcinoma (cSCC), can occur up to 200 times more in transplant patients compared to the general population [3–5]. Transplant recipients also experience more metastasis and more than 70% of the patients develop a subsequent cSCC within 5 years [6]. Although immunosuppressive treatment is recognized as an important risk factor for the development of cSCC after solid organ transplantation, little is known on the immune regulation leading up to formation of cSCC.

Most cSCCs are surrounded by immune cell infiltrates; however, these cells are incapable of mounting an effective immune response directed against the cSCC [7]. The role and phenotype of T cells surrounding an cSCC lesion has been studied extensively [8–10]; high numbers of forkhead box protein 3 $(FoxP3)^+$ regulatory T cells are associated with higher metastasis of cSCCs [11,12], whereas increased activity of effector and cytotoxic T cells often associates with better prognostic outcomes [13,14].

The function of cells, including T cells, is regulated by epigenetic mechanisms such as DNA methylation, which is the addition of a methyl group to a cytosine (C) followed by a guanine (G; CpG dinucleotide) in the DNA. DNA methylation controls gene expression, is a dynamic feature and can be influenced by environmental cues [15]. DNA methylation is also known to be dysregulated in disease such as cancer; however, it is often difficult to determine whether it is a driver or a consequence of the disease [16,17].

Here, we hypothesized that functional differences in circulating T cells represent risk factors in the development of a *de-novo* post-transplant cSCC. To address this hypothesis, we took an unbiased approach and performed genomewide DNA methylation analysis of circulating T cells after kidney transplantation but before the clinical onset of cSCC (discovery phase). DNA methylation profiles of kidney transplant recipients with a future cSCC were compared to those of matched kidney transplant recipients without cSCC. The prominent finding of this analysis was higher methylation of a region within *SERPINB9* in cSCC patients. SerpinB9 is an intracellular serine protease inhibitor that inhibits granzyme B [18,19], which is an important protease in the effector function of cytotoxic T cells by inducing apoptosis in target cells [20]. Cytotoxic T cells express serpinB9 to protect themselves against the activity of granzyme B, and studies have shown that high expression of serpinB9 in cytotoxic T cells makes them more potent killers [21,22]. Given these data, the finding on *SERPINB9* DNA methylation prompted us to further study *SERPINB9* methylation in a second cohort of kidney transplant recipients with recurrent cSCC, as well as the functional role of *SERPINB9* in cSCC on the level of mRNA and protein expression.

Materials and methods

Study design

Anonymized retrospective biobank samples were used in the discovery phase of the study; this included kidney transplant recipients before the diagnosis of their first post-transplant cSCC. A second cohort of patients was used to confirm findings from the discovery phase, and this included kidney transplant recipients during recurrent post-transplant cSCC. The use of biobank material and the inclusion of new patients was approved by the local medical ethical committee (MEC-2015-642). All kidney transplant recipients with a (future) post-transplant cSCC were matched to kidney transplant recipients who did not develop an cSCC within a similar time-period after the first transplant. Matching criteria included gender, age (± 4 years), ethnicity, cytomegalovirus (CMV) status and type of immunosuppressive drugs directly after transplantation. We included patients with at least one cSCC after transplantation and patients with cSCC *in situ* (Bowen's disease). Patients with another donor organ such as liver, heart or lung were excluded, as well as patients with a history of malignancy prior to transplantation. Non-cSCC patients with actinic keratosis, a precancerous lesion, were also excluded.

T cell isolation

Peripheral blood mononuclear cells (PBMCs) were isolated using standard Ficoll-Paque procedures. T cells were isolated from the PBMCs using fluorescence-activated cell sorting (FACS) with the BD FACSAria^{TM} II (BD Biosciences, San Jose, CA, USA). Total PBMCs were stained with CD3 Brilliant Violet 510 (Biolegend, San Diego, CA, USA), CD4 Pacific Blue (BD Biosciences), CD8 allophycocyanin-cyanin 7 (APC-Cy7) (BD Biosciences), CD45RO APC (Biolegend), CCR7 phycoerythrin (PE)-Cy7 (BD Biosciences), CD25 PE (BD Biosciences), CD127 fluorescein isothiocyanate (FITC) (eBioscience, Waltham, MA, USA) and to exclude non-viable cells Via-Probe 7-aminoactinomycin D (7AAD) (BD Biosciences) was used. After cell sorting the purities were > 96% for $CD3^+$ cells; samples below 95% were excluded for further analysis.

Genomewide DNA methylation arrays

Before isolating DNA from the T cells in the discovery cohort, all patient samples were randomized to minimize batch effects. DNA was isolated using the QIAamp DNA Micro kit (Qiagen, Venlo, the Netherlands), according to the manufacturer's protocol. Purity and concentration of the isolated DNA was assessed with the NanoDrop ND-8000 (Isogen Life Science, Utrecht, the Netherlands). DNA degradation was determined by gel electrophoresis. None of the samples showed a significant degradation.

The Infinium Human Methylation 450 arrays (Illumina, San Diego, CA, USA) were performed as described previously [23]. Data quality was examined using the MethylAid R package [24,25] and all samples passed quality controls using the default MethylAid thresholds. Probes with a detection *P*-value > 0·01, probes containing single nucleotide polymorphisms and probes on the sex chromosome were removed from the data set. A between-array normalization was applied to the types I and II probes separately using the DASEN method within the wateRmelon Bioconductor R package [25–27]. The methylation level of a CpG site is presented as a beta-value, a value between 0 (unmethylated) and 1 (fully methylated). After the quality controls and normalization, beta-values of 423 289 CpG sites remained for further analysis. Both the raw and normalized data are available via the NCBI Gene Expression Omnibus (GEO) database with Accession number GSE117050.

Data analysis DNA methylation arrays

To identify DNA methylation differences between the future cSCC and non-cSCC patients, we performed the data analysis as previously described [23]. First, a linear

mixed-effect model was performed using the lme4 R package [28]. The fixed effects included age, percentage of CD4, percentage of CD8 and CMV status. Percentages of CD4 and CD8 were included to correct for differences in T cell composition between individuals, and CMV is known to affect DNA methylation at specific genes [29]. Array IDs were included as a random effect to account for technical variation between the arrays. This resulted in single site-specific *P*-values and these *P*-values, together with their genomic location, were used as input into comb-p [30] to find differentially methylated regions (DMRs). A sliding window of 500 base pairs (bp) was used and the seed was set at $P < 0{\cdot}01$. A stringent multiple testing correction was applied using a Šidák correction (Šidák < 0·05) [31].

DNA methylation analysis by pyrosequencing

After the discovery phase we continued measuring DNA methylation of T cells with bisulphite pyrosequencing, an easy technique to quantitatively measure single-site DNA methylation [32], but first we tested whether pyrosequencing resulted in the same methylation values as the microarrays. Therefore, CpG sites within DMR 1 (*SERPINB9*) and DMR *2* (*VTRNA2-1*) were analysed in the same DNA samples that were used for the array analysis of 10 patients, a mixture of cSCC and non-cSCC patients.

Pyrosequencing was performed as described previously [23,33]. The polymerase chain reaction (PCR) primers, melting temperatures and amplicon sizes for the different PCR products can be found in the Supporting information, Table S1 together with the specific PCR programmes. For *SERPINB9,* 12 CpG sites, five of which were array probes, were sequenced in two separate reactions and DNA methylation was averaged per sequence reaction (regions 1 and 2). For *VTRNA2-1*, five CpG sites, three of which were array probes, were measured and an average of those five sites is presented in the results.

mRNA analysis

Total RNA was isolated from T cells using the High Pure RNA Isolation kit (Roche Applied Science, Pennsburg, Germany), according to the manufacturer's protocol. The quality and purity of the RNA was assessed using the NanoDrop ND-8000 (Isogen Life Science). Samples with a 260/280 ratio below 1·8 and a 260/230 ratio above 1 were excluded for further analysis. Messenger RNA (mRNA) of *SERPINB9* and *GRANZYME B (GZMB)* was quantified by real-time quantitative PCR (qPCR) using a Taqman gene expression assay. Primers used were Hs00394497_m1 (*SERPINB9*; Thermo Fisher Scientific, Waltham, MA, USA) and Hs01554355_m1 (*GZMB*; Thermo Fisher Scientific), glyceraldehyde 3-phosphate dehydrogenase (GAPDH) (Hs99999905_m1, Thermo Fisher Scientific) was used as housekeeping gene. qPCR was performed on the StepOnePlus Real-Time PCR system (Applied Biosystems). Gene expression was then calculated by transforming the cycle threshold (Ct) to cDNA copies (2^{40-Ct}). Dividing the number of *SERPINB9* and *GZMB* copies by the number of GAPDH copies resulted in a relative gene expression value.

Protein analysis

Protein levels of serpinB9 and granzyme B within T cells were assessed in cells before and after stimulation for 6 h at 37°C with or without α-CD3/CD28-coated Dynabeads® (Gibco, Waltham, MA, USA). The cells were measured by flow cytometry directly after defrosting the PBMCs. Monensin was added after 1 h of stimulation, whereby this newly synthesized granzyme B could be measured. CD107a APC (BD Biosciences) was added to the cell cultures to assess degranulation of the cells. Cells were stained with the following surface antibodies: CD3 Brilliant Violet 510 (Biolegend), CD4 APC-Cy7 (Biolegend), CD8 PE (Thermo Fisher Scientific) and Via-Probe 7AAD (BD Biosciences) was used to exclude non-viable cells. After surface staining the cells were fixed, permeabilized and stained for intracellular serpinB9 labelled with Alexa Fluor 488 (Bio-rad, Hercules, CA, USA) and granzyme B labelled with Brilliant Violet 421 (BD Biosciences). Isotype controls for AF488 (Bio-Rad) and BV421 (BD Biosciences) were used as negative controls for serpinB9 and granzyme B expression. The cells were then analysed on the FACSCanto ll (BD Biosciences) with FACSDiva software. Data were analysed blind, without knowledge of cSCC status of the samples, using Kaluza software 1.5a (Beckman Coulter, Brea, CA, USA).

Statistical analysis

Differences in clinical characteristics, DNA methylation, mRNA and protein expression between the cSCC and non-cSCC patients were statistically tested using SPSS version 21.0 (IBM Corp., Armonk, NY, USA). The Mann–Whitney *U*-test was used for the continuous variables and χ^2 test for the categorical variables. Data processing and statistical analysis of all the microarray data was performed in RStudio version 1.0.136 (RStudio Inc., Boston, MA, USA) with R version 3.2.5 [26]. Multiple testing correction of the microarray data was performed using a Šidák correction (Šidák < 0·05) [31]. Correlation between the DNA methylation levels quantified by pyrosequencing and the beta-values of the Illumina 450k arrays was calculated using Spearman's rank correlation coefficient using SPSS, as well as correlations between DNA methylation and mRNA expression. All statistical tests were two-tailed and a $P < 0{\cdot}05$ was considered statistically significant.

Results

Patients

The discovery cohort was comprised of 19 future cSCC and 19 non-cSCC patients who had been transplanted between 1997 and 2012. All patients in the discovery cohort were Caucasian European. No statistical differences were found between the patient characteristics of the future cSCC and non-cSCC patients (Table 1). The T cell subpopulations measured during FACS sorting were also not different between future cSCC and non-cSCC patients (data not shown). A detailed overview of the time between transplantation, sample and first diagnosis of cSCC can be found in the Supporting information, Fig. S1a.

The second cohort consisted of 37 non-cSCC and 45 cSCC patients during recurrent cSCC, who had been transplanted between 1976 and 2014. Six cSCC patients and five non-cSCC patients received a second kidney transplant. All patients in the second cohort were Caucasian European. There was a small statistical difference in the end-stage renal disease (ESRD) diagnosis between the cSCC and non-cSCC patients (P = 0·04; Table 2); no other statistical differences were found. The T cell subpopulations measured during FACS sorting were not different between cSCC and non-cSCC patients (data not shown). A detailed overview of the time between transplantation, sample and first diagnosis of cSCC can be found in the Supporting information, Fig. S1b.

Table 1. Patient characteristics of the discovery cohort before cSCC

	cSCC	Non-cSCC	
	n = 19	n = 19	
Age (years)[a]	64·8 (45–77)	63·5 (45–80)	P = 0·49
Gender (male)	14 (73·7%)	14 (73·7%)	P = 1
Years post-Tx[a]	1·5 (0·1–6·9)	1·3 (0·1–6·3)	P = 0·93
Years between Tx and first cSCC[a]	5·4 (0·9–12·5)	–	
Biopsy-proven rejection	–	3 (15·8%)	P = 0·07
Immunosuppressive treatment			
Induction therapy (ATG/basiliximab)	7 (36·8%)	5 (26·3%)	
Calcineurin inhibitors (tacrolimus/cyclosporin)	19 (100%)	18 (94·7%)	
Proliferation inhibitors (MMF/sirolimus)	18 (94·7%)	19 (100%)	
Anti-metabolites (azathioprine)	1 (5·3%)	–	
Corticosteriods	18 (94·7%)	19 (100%)	
HLA mismatches[a]	3·11 (0–6)	3·11 (0–6)	P = 0·94
CMV serostatus acceptor			P = 1
Negative	4 (21·1%)	4 (21·1%)	
Positive	15 (78·9%)	15 (78·9%)	
CMV serostatus donor			P = 0·11
Negative	12 (63·2%)	7 (36·8%)	
Positive	7 (36·8%)	12 (63·2%)	
ESRD diagnosis			P = 0·26
Polycystic kidney	7 (36·8%)	2 (10·5%)	
Hypertension	3 (15·8%)	6 (31·6%)	
Diabetic nephropathy	1 (5·3%)	1 (5·3%)	
Glomerulonephritis	1 (5·3%)	0 (0%)	
Other	7 (36·8%)	10 (52·6%)	
Dialysis pretransplantation			P = 0·49
Yes (PD/HD)	14 (73·7%)	12 (63·2%)	
No	5 (26·3%)	7 (36·8%)	

[a]Median and range.

cSCC = cutaneous squamous cell carcinoma; Tx = transplantation; ATG = anti-thymocyte globulin; MMF = mycophenolate mofetil; HLA = human leucocyte antigen; CMV = cytomegalovirus; ESDR = end-stage renal disease; PD = peritoneal dialysis; HD = haemodialysis.

Discovery of significant DMRs in circulating T cells before cSCC

To identify differentially methylated regions (DMRs) in circulating T cells associated with future cSCC development, we compared genomewide DNA methylation of kidney transplant recipients with and without a post-transplant cSCC, before the clinical onset of the cSCC. None of the single-site CpGs were statistically significant after multiple testing correction. However, we found seven regions significantly differentially methylated. In Table 3 the different DMRs, the genes annotated to these DMRs based on genomic location, the genomic location of the DMRs according to the hg19 genome build (UCSC Genome Browser), the number of probes (CpG sites on the array) within the regions and the effect size are presented. Of the significant DMRs, five were hypermethylated and two were hypomethylated in the future cSCC patients.

Genomic characteristics of DMR 1, 2 and 3

To understand the potential regulatory effect of the DMRs in T cells, the genomic location of the DMR and characteristics of that location are important. In Fig. 1, we visualized the top three DMRs with DNA methylation of both cSCC and non-cSCC patients expressed as beta-value, the genomic location of the DMRs and the primary T cell-specific chromatin state, which is a cell type-specific combination of epigenetic features obtained from the ROADMAP reference data [34]. DMR 1, annotated to *SERPINB9,* is located intragenically and within an actively transcribed region (Fig. 1a). DMR 2, annotated to VTRNA2-1, is located in the coding region and a bivalent/poised transcription start site (TSS) of the gene (Fig. 1b). DMR 3, also annotated to VTRNA2-1, is located further away from the *VTRNA2-1* gene, partly within a bivalent enhancer region and partly within a repressed area (Fig. 1b). All three DMRs overlap with a CpG island and those are often involved in the regulation of gene expression.

Table 2. Patient characteristics of the second cohort during cSCC

	cSCC	Non-cSCC	
	n = 45	*n* = 37	
Age (years)[a]	66·4 (34–84)	64·0 (28–75)	*P* = 0·20
Gender (male)	30 (66·7%)	25 (67·6%)	*P* = 0·93
Years post-Tx[a]	8·5 (0·4–40·5)	9·5 (0·1–35·9)	*P* = 0·89
Years between Tx and first cSCC[a]	4·7 (0–33)	–	
Biopsy proven rejection	12 (26·7%)	13 (35·1%)	*P* = 0·41
Immunosuppressive treatment			
Induction therapy (ATG/basiliximab)	1 (2·2%)	6 (16·2%)	
Calcineurin inhibitors (tacrolimus/ cyclosporin)	37 (82·2%)	34 (92%)	
Proliferation inhibitors (MMF/sirolimus)	27 (60%)	22 (59·5%)	
Anti-metabolites (azathioprine)	9 (20%)	4 (10·8%)	
Corticosteriods	44 (97·8%)	37 (100%)	
HLA mismatches[a]	3·0 (0–6)	3·0 (0–6)	*P* = 0·86
CMV serostatus acceptor			*P* = 0·74
Negative	17 (37·8%)	11 (29·7%)	
Positive	22 (48·9%)	20 (54·1%)	
Unknown	6 (13·3%)	6 (16·2%)	
CMV serostatus donor			*P* = 0·62
Negative	15 (33·3%)	14 (37·8%)	
Positive	18 (40%)	11 (29·7%)	
Unknown	12 (26·7%)	12 (32·4%)	
ESRD diagnosis			*P* = 0·04
Polycystic kidney	11 (24·4%)	5 (13·5%)	
Hypertension	8 (17·8%)	7 (18·9%)	
Diabetic nephropathy	–	7 (18·9%)	
Glomerulonephritis	7 (15·6%)	4 (10·8%)	
Other	19 (42·2%)	14 (37·8%)	
Dialysis pretransplantation			*P* = 0·83
Yes (PD/HD)	22 (48·9%)	19 (51·4%)	
No	23 (51·1%)	18 (48·6%)	

[a]Median and range.

cSCC = cutaneous squamous cell carcinoma; Tx = transplantation; ATG = anti-thymocyte globulin; MMF = mycophenolate mofetil; HLA = human leucocyte antigen; CMV = cytomegalovirus; ESDR = end-stage renal disease; PD = peritoneal dialysis; HD = haemodialysis.

Confirmation of microarray methylation values by pyrosequencing

To confirm that the above-described findings can also be found with a different technique, DNA methylation of DMRs 1 and 2 was measured by pyrosequencing in the same DNA samples. Correlation between DNA methylation values obtained with the microarray and pyrosequencing was strong in both DMRs (Supporting information, Fig. S2). Spearman's *r* for *SERPINB9* was 0·86 ($P < 0·0001$) and for *VTRNA2-1* Spearman's *r* was 0·96 ($P < 0·0001$). As a result of this strong correlation, we measured DNA methylation with pyrosequencing throughout the rest of the study.

High intragenic SERPINB9 methylation during cSCC

To assess the stability of the DNA methylation profiles identified before the development of cSCC, we included a second patient cohort during recurrent cSCC (Table 2). *VTRNA2-1* was measured and was not significantly different between cSCC and non-cSCC patients (data not shown). When *SERPINB9* was measured, it was significantly different between cSCC and non-cSCC patients. Median DNA methylation of *SERPINB9* was 58·7% (range: 32·5–81·3%) for region 1 and 54·4% (30·0–78·5%) for region 2 in the cSCC patients and 50·2% (21·8–77·5%) for region 1 and 46·4% (22·1–74·0%) for region 2 in the non-cSCC patients (region 1: $P = 0·004$; region 2: $P = 0·008$) (Fig. 2).

Similarly to our discovery cohort, cSCC patients demonstrated higher *SERPINB9* methylation values than non-cSCC patients. In addition, serpinB9 has a strong relation to T cell function as a regulator of cytotoxicity [21,22]. Together, these findings warranted further investigation into the role of *SERPINB9* in controlling the cytotoxic T cells that are key for immunosurveillance in post-transplant cSCC.

mRNA expression negatively correlates to DNA methylation only in the non-cSCC patients

To study the translation from DNA to protein of serpinB9, we analysed mRNA expression of *SERPINB9* in T cells. Relative mRNA expression of *SERPINB9* was not significantly different between cSCC ($n = 30$) and non-cSCC patients ($n = 27$; Fig. 3a). When we zoomed in and studied the correlation between DNA methylation and mRNA expression of *SERPINB9* in the total patient population this was statistically significant ($P = 0.004$, Fig. 3b). However, when we stratified the data by cSCC status, the correlation remained significant only in the non-cSCC patients ($P = 0·0003$; Fig. 3c,d) and not in the cSCC patients, indicating a disrupted transcriptional regulation in the cSCC patients.

Lower serpinB9 expression in circulating T cells of cSCC patients

To investigate the functional impact of differentially methylated *SERPINB9* on cytotoxicity, we analysed the expression of the following markers: granzyme B (inhibited by serpinB9) and degranulation of T cells by CD107a expression before and after stimulation. Gating strategies for granzyme B and CD107a are presented in the Supporting information, Fig. S3. The percentage of $CD3^+$ granzyme

Table 3. Resulting differentially methylated regions of the discovery analysis

	Annotated to:	Genomic location (hg19)	Length DMR	No. of probes	Function	Regional *P*-value	Effect size	DMR state
1	*SERPINB9*	chr6:2891973–2892153	180 bp	5	Granzyme B inhibitor	$1{\cdot}09 \times 10^{-13}$	0·14	Hyper
2	*VTRNA2-1*	chr5:135415948–135416614	666 bp	12	Inhibitor of protein kinase R	$1{\cdot}40 \times 10^{-10}$	0·11	Hyper
3	*VTRNA2-1*	chr5:135414858–135415259	401 bp	4	Inhibitor of protein kinase R	$1{\cdot}90 \times 10^{-8}$	0·07	Hyper
4	*PIF1*	chr15:65116194–65116558	364 bp	3	ATP metabolism	$1{\cdot}36 \times 10^{-7}$	–0·05	Hypo
5	*APC2*	chr19:1465962–1466163	201 bp	2	Signalling pathway regulation	$1{\cdot}48 \times 10^{-7}$	0·08	Hyper
6	*RPH3AL*	chr17:151914–152351	437 bp	6	Tumour suppressor	$3{\cdot}39 \times 10^{-7}$	–0·07	Hypo
7	*AC144450.2*	chr2:1609660–1609833	173 bp	2	LincRNA	$3{\cdot}15 \times 10^{-6}$	0·08	Hyper

DMR = differentially methylated region; chr = chromosome; bp = base pair.

B^+ cells was not significantly different between the cSCC patients and non-cSCC patients (Supporting information, Fig. S4a), nor was degranulation of the T cells, as determined by CD107a staining (Supporting information, Fig. S4b).

SerpinB9 expression was also measured in the T cells. Gating strategy for serpinB9 is presented in the Supporting information, Fig. S5. The percentage of $CD3^+$ $serpinB9^+$ cells before stimulation was not significantly different between cSCC and non-cSCC patients (Fig. 4a). After stimulation, serpinB9 expression in all T cells was upregulated to 98·2% (93·0–99·0%) for the cSCC patients and 99·1% (97·2–99·7%) for the non-cSCC patients, and this was significantly different even though the differences were small ($P = 0{\cdot}006$; Fig. 4b). When analysing serpinB9 expression in the $CD4^+$ and $CD8^+$ population separately, we observed that the percentage of $CD4^+$ $serpinB9^+$ cells was significantly lower in the cSCC patients than in the non-cSCC patients after stimulation (Fig. 4c). In the $CD8^+$ population this difference was not observed (Fig. 4d). These results show that the $CD4^+$ population is the main contributor to the difference observed in the total T cell population.

Discussion

In this study, we demonstrate high DNA methylation of *SERPINB9* in circulating T cells before the clinical onset of cSCC in kidney transplant recipients and, in a different patient cohort, during recurrent post-transplant cSCC. These data identify high DNA methylation of *SERPINB9* as a novel risk factor for development of both *de-novo* and subsequent post-transplant cSCC. In addition, T cells of cSCC patients were unable to fully upregulate serpinB9 expression *in vitro*, which might provide insight into the role of the peripheral immune system in the development of an cSCC in kidney transplant recipients.

In a previous study, where we identified DMRs associated with post-transplant cSCC before transplantation [23], *SERPINB9* was not significantly different between T cells of future cSCC patients and non-cSCC patients. Thus, differences in *SERPINB9* DNA methylation that identify patients at risk for cSCC arise after kidney transplantation. Kidney transplantation and the use of immunosuppressive therapy probably affect DNA methylation profiles of the T cells [35]. However, as we demonstrated high *SERPINB9* methylation in patients before and after the development of a *de-novo* post-transplant cSCC, it seems a persistent risk factor for cSCC after transplantation.

Based on the differential DNA methylation of *SERPINB9,* one could expect differences in mRNA expression of *SERPINB9*. Nevertheless, when *SERPINB9* mRNA expression was measured in the T cells, this was not significantly different between cSCC patients and non-cSCC patients. This is comparable to findings by Ryer *et al*. [36], who identified higher methylation of the same region within *SERPINB9* in PBMCs of patients with abdominal aortic aneurysm. Despite the differential DNA methylation, they also did not detect a difference in mRNA expression. This is due most probably to the intragenic location of the DMR, outside the promoter region of *SERPINB9*. The effect of intragenic DNA methylation on gene expression is still debated [37], although in this study we demonstrated an inverse correlation between intragenic *SERPINB9* DNA methylation and mRNA expression in the T cells of non-cSCC patients. Surprisingly, this inverse correlation was absent in the T cells of cSCC patients. This illustrates a disturbed transcriptional regulation of *SERPINB9* in cSCC patients and a clear difference between these two patient groups.

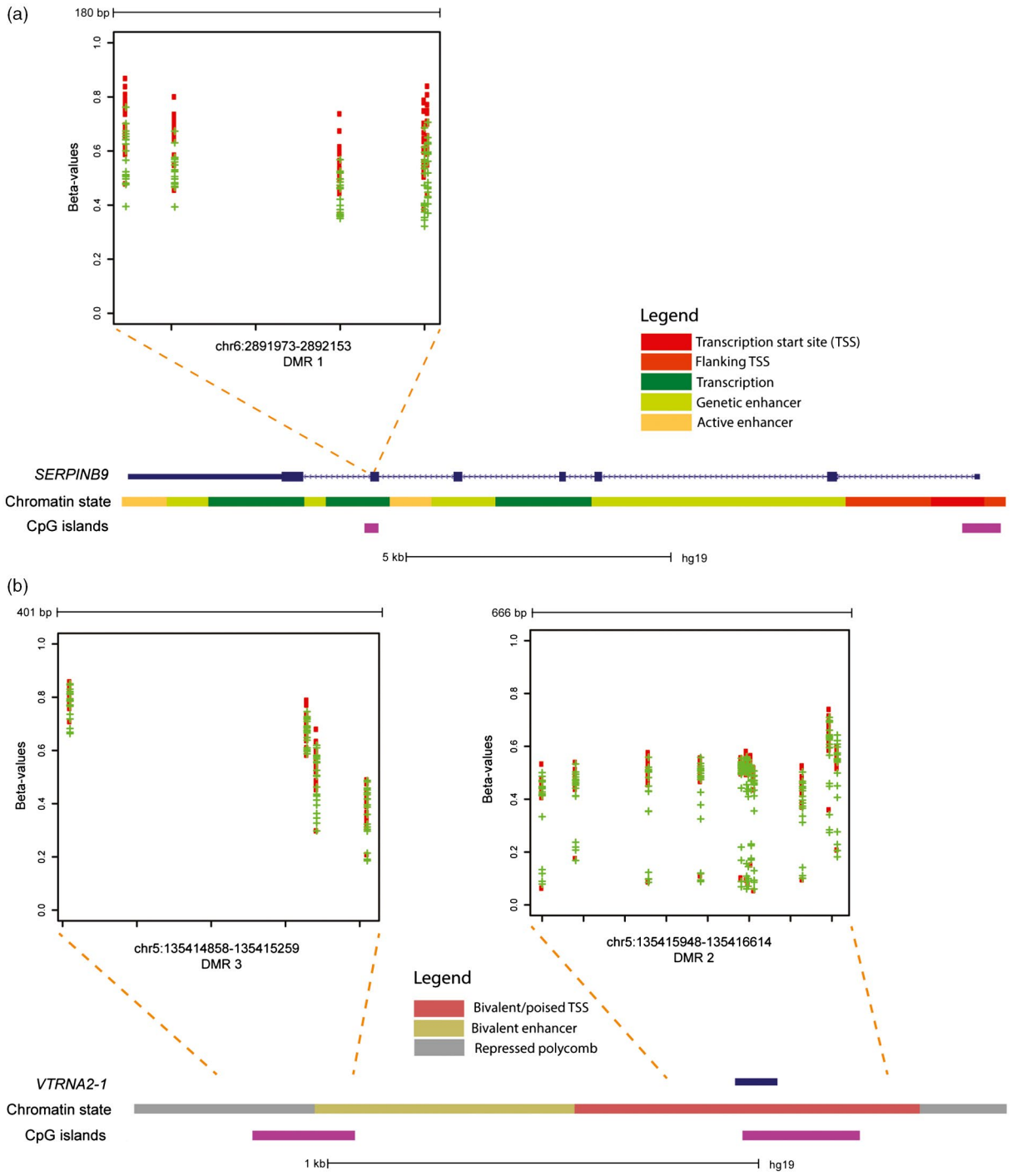

Fig. 1. Genomic characteristics of differentially methylated regions (DMR) 1–3. The chromatin state specific for primary T cells of *SERPINB9* (a) and *VTRNA2-1* (b) is depicted with the cytosine–phosphate–guanine (CpG) islands below in purple. The location of the DMRs are highlighted by the orange dotted lines. The graphs present the raw beta-values (*y*-axis) and the genomic location of the single CpGs (*x*-axis), cutaneous squamous cell carcinoma (cSCC) patients are depicted in red and the non-cSCC in green. The transcription start site (TSS) is the promoter of a gene; enhancers are locations that bind gene-activating or repressing proteins such as transcription factors and repressed polycomb represents inactive DNA.

Previous studies have shown that higher expression of serpinB9 increased the potency of cytotoxic T cells [21,22]. We observed a slightly lower expression of serpinB9 in the T cells of our cSCC patients, which was due mainly to the CD4 compartment of the T cells, although it is questionable whether a difference

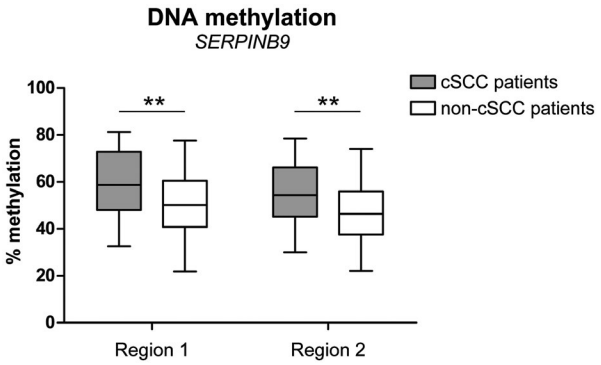

Fig. 2. DNA methylation in T cells of cutaneous squamous cell carcinoma (cSCC) and non-cSCC patients for regions 1 and 2 of *SERPINB9* measured by pyrosequencing. $^{**}P < 0{\cdot}01$.

between 98 and 99% serpinB9-positive cells is biologically relevant. In addition, the regulation of serpinB9 seems independent from the regulation of cytotoxic markers of T cells, as we did not identify differences in the expression of granzyme B and CD107a between cSCC patients and non-cSCC patients. SerpinB9 is an intracellular protein inactivating granzyme B once it is released into the cytoplasm [38], and therefore serpinB9 exerts its effect on cytotoxicity only after granzyme B is synthesized to its active form. The absence of differences in cytotoxicity which, in most cases, is restricted to the $CD8^+$ T cells, and the *SERPINB9* DNA methylation difference in the $CD4^+$ T cells may lead to the conclusion that the $CD4^+$ T cells are the population of interest in post-transplant cSCC.

DNA methylation of *SERPINB9* might represent a future treatment target for cSCC in transplant recipients. It would be interesting to decrease *SERPINB9* DNA methylation in cSCC patients to the level observed in non-cSCC patients and study whether that affects future cSCC development in those patients. DNA methylation can be edited by use of the CRISPR/cas9 system, a technique called 'epigenetic editing' [39]. Although this novel technology is far from a clinical application, it is a promising concept for the future. Additionally, this approach will reveal whether

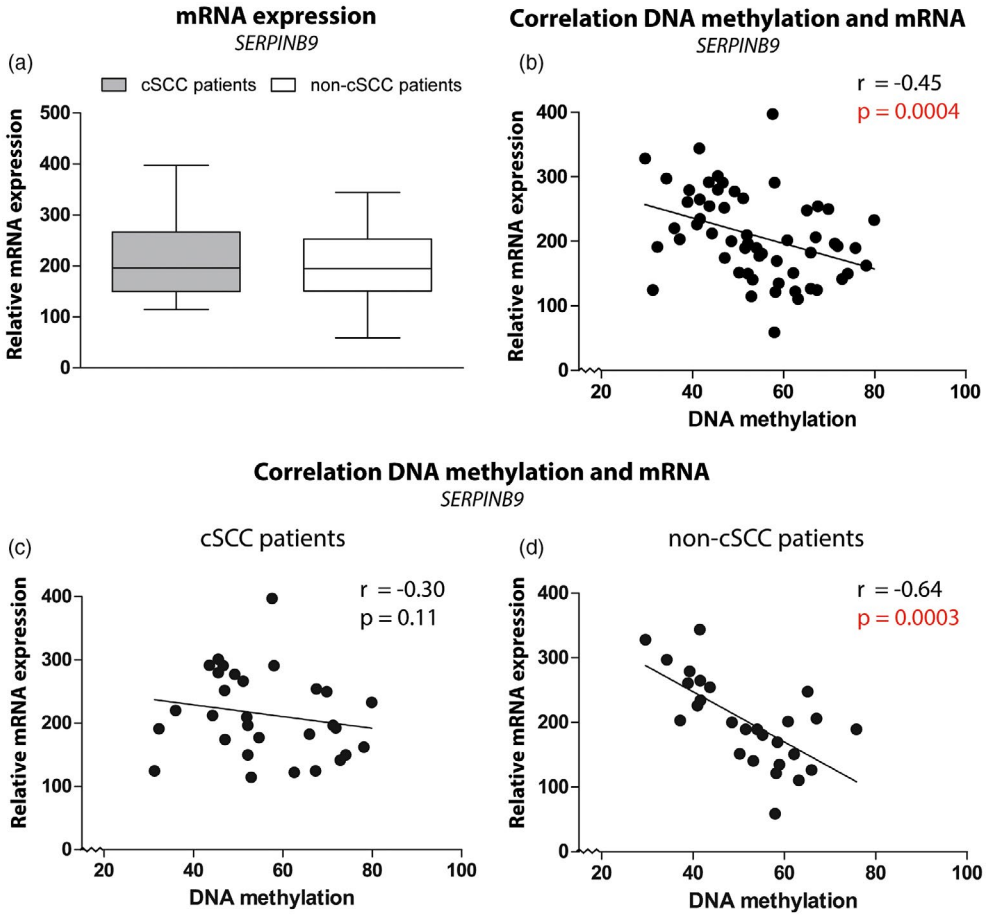

Fig. 3. Relative mRNA expression of *SERPINB9* (a) in cutaneous squamous cell carcinoma (cSCC) *versus* non-cSCC patients, (b) as correlated to *SERPINB9* DNA methylation (*x*-axis) within all patients, (c) within the cSCC patients and (d) within the non-cSCC patients.

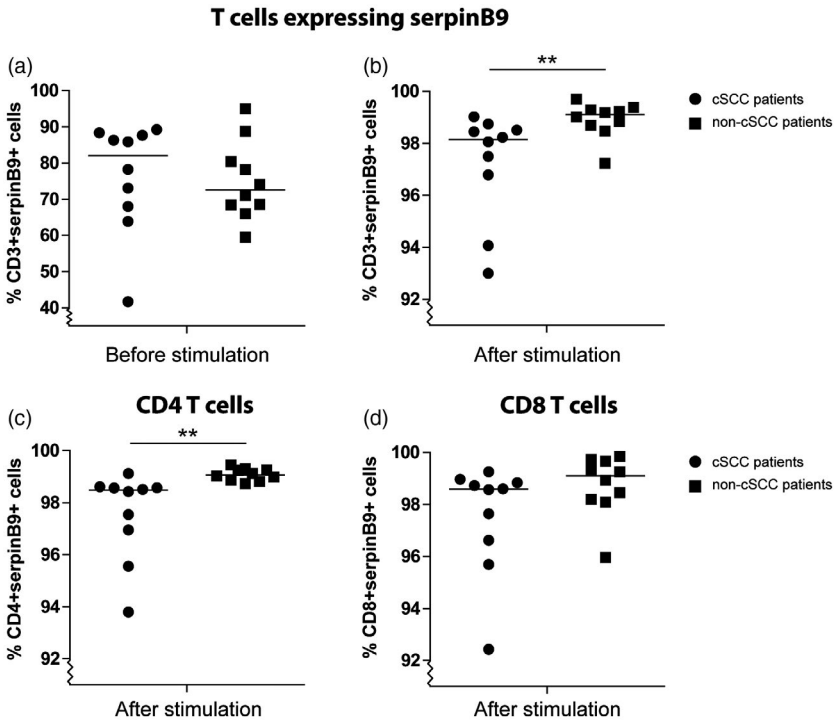

Fig. 4. Quantified flow cytometry data on serpinB9 expression by T cells. (a) Percentage of T cells that expressed serpinB9 before stimulation in the cutaneous squamous cell carcinoma (cSCC) and non-cSCC patients and (b) after stimulation. (c) Percentage of CD4 T cells and (d) CD8 T cells that expressed serpinB9 after stimulation in the cSCC and non-cSCC patients. $^{**}P < 0{\cdot}01$.

SERPINB9 DNA methylation plays a causal role in cSCC development or whether it is a consequence of another, as yet unknown, mechanism leading to post-transplant cSCC development.

We are aware that the single-centre design and small sample size may be a limitation of this study. Details such as sun exposure were unknown, and dosages of immunosuppression were often adjusted or immunosuppressive regimens were changed during the course of post-transplant treatment. It was therefore not possible to take these factors into account. Nevertheless, we show a promising proof-of-concept that studying DNA methylation of *SERPINB9* in peripheral T cells can identify kidney transplant recipients at risk for cSCC. The disturbed transcriptional regulation of *SERPINB9* and the lower protein expression of serpinB9 warrant further investigation to fully understand the relation with cSCC development in kidney transplant recipients.

Together, these findings demonstrate that DNA methylation, transcriptional regulation and protein expression of serpinB9 differ between cSCC and non-cSCC patients. This identifies a novel risk factor for the development of post-transplant cSCC and may provide mechanistic insight into the role of circulating T cells in cSCC development. Future studies will identify whether serpinB9 plays a causal role in cSCC development and if it is a suitable treatment target to prevent cSCC development after kidney transplantation.

Acknowledgements

F. P. contributed to designing, performing and analysing the experiments, interpreting the results and writing of the manuscript; A. P. performed the experiments; T. B. and A. M. contributed to interpretation of the results; J. W. reviewed the manuscript; M. B. contributed to interpreting the results and reviewed the manuscript; and C. B. and K. B. both contributed to designing the experiments, interpreting the results and writing of the manuscript. All authors read and approved the final manuscript. The authors would like to thank R. Kraaijeveld and W. Verschoor for performing all the FACS sorting experiments, M. Verbiest for performing the microarray experiments, P. Mandaviya for her advice on the R data analysis and L. Hofland for providing the pyrosequencing machine.

Disclosures

The authors declare no conflicts of interest. No funding was received for this study.

References

1 Vajdic CM, van Leeuwen MT. Cancer incidence and risk factors after solid organ transplantation. Int J Cancer 2009; **125**:1747–54.

2 van de Wetering J, Roodnat JI, Hemke AC, Hoitsma AJ, Weimar W. Patient survival after the diagnosis of cancer in renal transplant recipients: a nested case–control study. Transplantation 2010; **90**:1542–6.

3 Mittal A, Colegio OR. Skin cancers in organ transplant recipients. Am J Transplant 2017; **17**:2509–30.

4 Hanlon A, Colegio OR. The cutting edge of skin cancer in transplant recipients: scientific retreat of international transplant skin cancer collaborative and skin cancer in organ transplant patients Europe. Am J Transplant 2014; **14**:1012–5.

5 Bouwes Bavinck JN, Feltkamp MCW, Green AC *et al*. Human papillomavirus and posttransplantation cutaneous squamous cell carcinoma: a multicenter, prospective cohort study. Am J Transplant 2018; **18**:1220–30.

6 Wisgerhof HC, Edelbroek JR, de Fijter JW *et al*. Subsequent squamous- and basal-cell carcinomas in kidney-transplant recipients after the first skin cancer: cumulative incidence and risk factors. Transplantation 2010; **89**:1231–8.

7 Oleinika K, Nibbs RJ, Graham GJ, Fraser AR. Suppression, subversion and escape: the role of regulatory T cells in cancer progression. Clin Exp Immunol 2013; **171**:36–45.

8 Feldmeyer L, Ching G, Vin H *et al*. Differential T-cell subset representation in cutaneous squamous cell carcinoma arising in immunosuppressed versus immunocompetent individuals. Exp Dermatol 2016; **25**:245–7.

9 Bauer C, Abdul Pari AA, Umansky V *et al*. T-lymphocyte profiles differ between keratoacanthomas and invasive squamous cell carcinomas of the human skin. Cancer Immunol Immunother 2018; **67**:1147–57.

10 Crespo E, Fernandez L, Lucia M *et al*. Effector antitumor and regulatory T cell responses influence the development of nonmelanoma skin cancer in kidney transplant patients. Transplantation 2017; **101**:2102–10.

11 Lai C, August S, Albibas A *et al*. OX40+ regulatory T cells in cutaneous squamous cell carcinoma suppress effector T-cell responses and associate with metastatic potential. Clin Cancer Res 2016; **22**:4236–48.

12 Clark RA, Huang SJ, Murphy GF *et al*. Human squamous cell carcinomas evade the immune response by down-regulation of vascular E-selectin and recruitment of regulatory T cells. J Exp Med 2008; **205**:2221–34.

13 Gajewski TF, Schreiber H, Fu Y-X. Innate and adaptive immune cells in the tumor microenvironment. Nat Immunol 2013; **14**:1014–22.

14 Mahmoud SM, Paish EC, Powe DG *et al*. Tumor-infiltrating CD8+ lymphocytes predict clinical outcome in breast cancer. J Clin Oncol 2011; **29**:1949–55.

15 Feil R, Fraga MF. Epigenetics and the environment: emerging patterns and implications. Nat Rev Genet 2012; **13**:97–109.

16 Jones MJ, Fejes AP, Kobor MS. DNA methylation, genotype and gene expression: who is driving and who is along for the ride? Genome Biol 2013; **14**:126.

17 Feinberg AP. The key role of epigenetics in human disease prevention and mitigation. N Engl J Med 2018; **378**:1323–34.

18 Kaiserman D, Bird PI. Control of granzymes by serpins. Cell Death Differ 2010; **17**:586–95.

19 Classen CF, Bird PI, Debatin KM. Modulation of the granzyme B inhibitor proteinase inhibitor 9 (PI-9) by activation of lymphocytes and monocytes *in vitro* and by Epstein–Barr virus and bacterial infection. Clin Exp Immunol 2006; **143**:534–42.

20 Heusel JW, Wesselschmidt RL, Shresta S, Russell JH, Ley TJ. Cytotoxic lymphocytes require granzyme B for the rapid induction of DNA fragmentation and apoptosis in allogeneic target cells. Cell 1994; **76**:977–87.

21 Hirst CE, Buzza MS, Bird CH *et al*. The intracellular granzyme B inhibitor, proteinase inhibitor 9, is up-regulated during accessory cell maturation and effector cell degranulation, and its overexpression enhances CTL potency. J Immunol 2003; **170**:805–15.

22 Azzi J, Ohori S, Ting C *et al*. Serine protease inhibitor-6 differentially affects the survival of effector and memory alloreactive CD8–T cells. Am J Transplant 2015; **15**:234–41.

23 Peters FS, Peeters AMA, Mandaviya PR *et al*. Differentially methylated regions in T cells identify kidney transplant patients at risk for *de novo* skin cancer. Clin Epigenetics 2018; **10**:81.

24 van Iterson M, Tobi EW, Slieker RC *et al*. MethylAid: visual and interactive quality control of large Illumina 450k datasets. Bioinformatics 2014; **30**:3435–7.

25 Huber W, Carey VJ, Gentleman R *et al*. Orchestrating high-throughput genomic analysis with Bioconductor. Nat Methods 2015; **12**:115–21.

26 RCoreTeam. R: A Language and Environment for Statistical Computing. Vienna, Austria: R Foundation for Statistical Computing; 2016.

27 Pidsley R, Wong CCY, Volta M, Lunnon K, Mill J, Schalkwyk LC. A data-driven approach to preprocessing Illumina 450K methylation array data. BMC Genom 2013; **14**:293.

28 Bates D, Mächler M, Bolker B, Walker S. Fitting linear mixed-effects models using lme4. J Stat Softw 2015; **67**:48.

29 Boer K, de Wit LEA, Peters FS *et al*. Variations in DNA methylation of interferon gamma and programmed death 1 in allograft rejection after kidney transplantation. Clin Epigenetics 2016; **8**:116.

30 Pedersen BS, Schwartz DA, Yang IV, Kechris KJ. Comb-p: software for combining, analyzing, grouping and correcting spatially correlated P-values. Bioinformatics 2012; **28**:2986–8.

31 Šidák Z. Rectangular confidence regions for the means of multivariate normal distributions. J Am Stat Assoc 1967; **62**:626–33.

32 Tost J, Gut IG. DNA methylation analysis by pyrosequencing. Nat Protoc 2007; **2**:2265–75.

33 Peters FS, Peeters AMA, Hofland LJ, Betjes MGH, Boer K, Baan CC. Interferon-gamma DNA methylation is affected by mycophenolic acid but not by tacrolimus after T-cell activation. Front Immunol 2017; **8**:822.
34 Roadmap Epigenomics Consortium, Kundaje A, Meuleman W *et al*. Integrative analysis of 111 reference human epigenomes. Nature 2015; **518**:317–30.
35 Chu AY, Tin A, Schlosser P *et al*. Epigenome-wide association studies identify DNA methylation associated with kidney function. Nat Commun 2017; **8**:1286.
36 Ryer EJ, Ronning KE, Erdman R *et al*. The potential role of DNA methylation in abdominal aortic aneurysms. Int J Mol Sci 2015; **16**:11259–75.
37 Jones PA. Functions of DNA methylation: islands, start sites, gene bodies and beyond. Nat Rev Genet 2012; **13**:484–92.
38 Heutinck KM, ten Berge IJ, Hack CE, Hamann J, Rowshani AT. Serine proteases of the human immune system in health and disease. Mol Immunol 2010; **47**:1943–55.
39 de Groote ML, Verschure PJ, Rots MG. Epigenetic editing: targeted rewriting of epigenetic marks to modulate expression of selected target genes. Nucleic Acids Res 2012; **40**:10596–613.

Supporting Information

Additional supporting information may be found in the online version of this article at the publisher's web site:

Fig. S1. Detailed time schedule of (a) the discovery patient cohort and (b) the second patient cohort. On the Y-axis are all the cSCC patients and their matched controls and on the X-axis is the time in months from the transplantation (Tx) onwards.

Fig. S2. Correlation between methylation values obtained by pyrosequencing and microarray. (a) XY plot of DMR 1 (*SERPINB9*) with array values on the X-axis and pyro values on the Y-axis. (b) Detailed graph for each of the 5 sites within DMR 1 (*SERPINB9*) with in red the cSCC patients and in green the non-cSCC patients. (c) XY plot of DMR 2 (*VTRNA2-1*) with pyro values on the X-axis and array values on the Y-axis. (d) Detailed graph for each of the 3 sites within DMR 2 (*VTRNA2-1)* with in red the cSCC patients and in green the non-cSCC patients.

Fig. S3. Gating strategy for granzyme B expression and CD107a by T cells. Representative examples of (a) lymphocyte gate from forward scatter (FSC) and sideward scatter (SSC), (b) living T cells gated from 7AAD-CD3 staining, (c) granzyme B+ cells gated within the living T cells at 0 hours, (d) granzyme B+ cells gated within the living T cells at 6 hours, (e) CD107a+ cells gated within the living T cells at 0 hours, (f) CD107a+ cells gated within the living T cells at 6 hours, (g) isotype control in green and granzyme B stained sample in red at 0 hours and (h) isotype control in green and granzyme B stained sample in red at 6 hours.

Fig. S4. Quantified flow cytometry data on granzyme B and CD107a expression by T cells. (a) Percentage of T cells that expressed granzyme B before and after stimulation in the cSCC and non-cSCC patients. (b) Percentage of T cells that expressed CD107a before and after stimulation in the cSCC and non-cSCC patients.

Fig. S5. Gating strategy for serpinB9 expression by T cells. Representative examples of (a) lymphocyte gate from forward scatter (FSC) and sideward scatter (SSC), (b) living T cells gated from 7AAD-CD3 staining, (c) serpinB9+ cells gated within the living T cells at 0 hours, (d) serpinB9+ cells gated within the living T cells at 6 hours, (e) isotype control in green and serpinB9 stained sample in red at 0 hours and (f) isotype control in green and serpinB9 stained sample in red at 6 hours.

Table S1. PCR and sequence primers of genes for validation.

